Book Chapter

Development of a Rapid Mass Spectrometric Determination of AMP and Cyclic AMP for PDE3 Activity Study: Application and Computational Analysis for Evaluating the Effect of a Novel 2-oxo-1,2-dihydropyridine-3-carbonitrile Derivative as PDE-3 Inhibitor

Ilaria Cicalini[1,2†], Barbara De Filippis[3†], Nicola Gambacorta[4], Antonio Di Michele[3], Silvia Valentinuzzi[1,3], Alessandra Ammazzalorso[3], Alice Della Valle[3], Rosa Amoroso[3], Orazio Nicolotti[4], Piero Del Boccio[1,3‡] and Letizia Giampietro[3*‡]

[1]Centre of Advanced Studies and Technologies (CAST), University "G. d'Annunzio" of Chieti-Pescara, Italy
[2]Department of Medicine and Aging Sciences, University "G. d'Annunzio" of Chieti-Pescara, Italy
[3]Department of Pharmacy, University "G. d'Annunzio" of Chieti-Pescara, Italy
[4]Department of Farmacia-Scienze del Farmaco, University "A. Moro" of Bari, Italy

[†]These authors contributed equally to this work.
[‡]Both co-authors acted as senior investigators and should be considered equal "last authors".

***Corresponding Author:** Letizia Giampietro, Department of Pharmacy, University "G. d'Annunzio" of Chieti-Pescara, 66100 Chieti, Italy

Published **December 23, 2020**

This Book Chapter is a republication of an article published by Letizia Giampietro, et al. at Molecules in April 2020. (Cicalini, I.; De Filippis, B.; Gambacorta, N.; Di Michele, A.;

Valentinuzzi, S.; Ammazzalorso, A.; Della Valle, A.; Amoroso, R.; Nicolotti, O.; Del Boccio, P.; Giampietro, L. Development of a Rapid Mass Spectrometric Determination of AMP and Cyclic AMP for PDE3 Activity Study: Application and Computational Analysis for Evaluating the Effect of a Novel 2-oxo-1,2-dihydropyridine-3-carbonitrile Derivative as PDE-3 Inhibitor. Molecules 2020, 25, 1817.)

How to cite this book chapter: Ilaria Cicalini, Barbara De Filippis, Nicola Gambacorta, Antonio Di Michele, Silvia Valentinuzzi, Alessandra Ammazzalorso, Alice Della Valle, Rosa Amoroso, Orazio Nicolotti, Piero Del Boccio, Letizia Giampietro. Development of a Rapid Mass Spectrometric Determination of AMP and Cyclic AMP for PDE3 Activity Study: Application and Computational Analysis for Evaluating the Effect of a Novel 2-oxo-1,2-dihydropyridine-3-carbonitrile Derivative as PDE-3 Inhibitor. In: Sławomir Lach, editor. Prime Archives in Molecular Sciences. Hyderabad, India: Vide Leaf. 2020.

Abstract

A simple, quick, easy and cheap tandem mass spectrometry (MS/MS) method for the determination of AMP and cAMP has been newly developed. This novel MS/MS method was applied for the evaluation of the inhibitory effect of a novel 2-oxo-1,2-dihydropyridine-3-carbonitrile derivative, also named DF492, on PDE3 enzyme activity in comparison to its parent drug Milrinone. Molecule DF492, with an IC_{50} of 409.5 nM, showed an inhibition of PDE3 greater than Milrinone (IC_{50} = 703.1 nM). To explain the inhibitory potential of DF492, molecular docking studies toward the human PDE3A have been carried out with the aim of predicting the binding mode of the DF492. The presence of different decorating bulkier fragments in DF492 was pursued

to shift affinity of this novel molecule toward PDE3A compared to Milrinone in according to both theoretical and experimental results. The described Mass Spectrometric approach could have a wider potential use in kinetic and biomedical studies and could be applied for the determination of other phosphodiesterase inhibitor molecules.

Keywords

Phosphodiesterases Activity; AMP; Cyclic AMP; Tandem Mass Spectrometry; Dihydropyridine; Docking Studies

Introduction

3',5'-cyclic adenosine monophosphate (cAMP) and 3',5'-cyclic guanosine monophosphate (cGMP) are intracellular second messengers that play a key role in many physiological processes. cAMP is synthesized from ATP by adenylate cyclase (AC) and cGMP is synthesized by guanylate cyclase (GC) and they are metabolized and degraded by cyclic nucleotide phosphodiesterases (PDEs) [1, 2].

Since 1970s, different isoforms of PDEs have been described in mammalians and these are grouped into 11 families based on structural similarity (PDE1-PDE11). PDEs are inhibited by different drugs blocking one or more PDE subtypes. PDE3 is described as a phosphodiesterase isoform involved in cardiovascular disease. This isoform comprises two subfamilies: PDE3A and PDE3B showing different subcellular and tissue distributions. PDE3A is highly expressed in cardiovascular system and it is subtype more abundant in platelet [3] while PDE3B is mainly present in adipocytes [4].

The inhibition of PDE3 increases the intracellular levels of cAMP and consequently the force of heart contractions. Milrinone is a specific PDE3A inhibitor and it is generally used to treat acute congestive heart failure, pulmonary hypertension, or chronic heart failure [5].This drug has cardioprotective effects associated with an increase of heart muscle contraction, vasodilatation and reduction of inflammatory damage produced

by tumor necrosis factor-alpha (TNF-alpha) [6]. Milrinone has also been reported to reduce Ischemia-Reperfusion Injury to the rat heart [7], lung [8] and liver [9].

Moreover, several studies demonstrated that Milrinone has the capability to decrease the apoptosis and the releasing of free oxygen radicals, with a consequent anti-inflammatory effect [10-12].

Vasodilatation, anti-inflammatory, and antiaggregant effects of Milrinone on regulating the microcirculation cause an increase of tissue perfusion [13].

Likewise, Milrinone increases the calcium entry into the cell by activating the calcium sensitive signaling cascades, resulting in a considerable neuroprotective effect on ischemic brain [14]. Milrinone has also emerged as an option to treat delayed cerebral ischemia after subarachnoid haemorrhage [15]. During the last years, Milrinone has claimed interest especially for an innovative use as intravenous salvage therapy in acute internal carotid artery use [16].

In the past, several chemical modifications of Milrinone have been done in order to synthesize new inotropic compounds with best cardiotonic activity and fewer side effects [17-23]. These chemical modifications were carried out following important information revealed by PDE3B crystal structure [16].

The interesting results obtained prompted us to investigate new Milrinone analogues in order to enlarge our knowledge about Milrinone Structure-Activity Relationship (SAR). For these reasons we synthesized new compounds with modifications at the 3-position of Milrinone, where the 4-pyridyl moiety was simply removed or replaced with an acid, ester or amide group [24]. All compounds were tested to evaluate the intracellular calcium increase in single livingH9C2 cardiac cells. Among them, only amide derivative DF492, at concentration of 10 μM in the presence of the KCl dependent $[Ca^{2+}]_i$ transient of cardiac myocytes, is able to extend it in a significant manner (Figure 1).

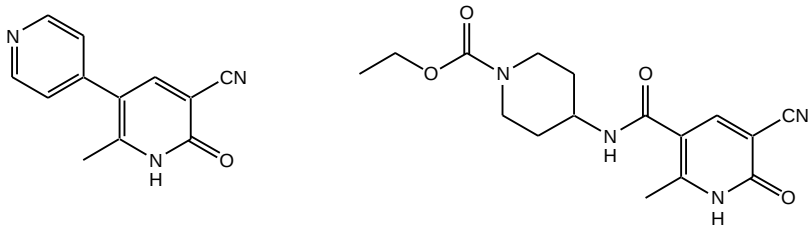

milrinone **DF492**

Figure 1: Chemical structures of Milrinone and new analogue DF492.

To date, the most applied methods for the indirect measurement of PDE3 activity regard the quantification of cAMP by using immunological assay. However, this kind of analytical techniques may require an acetylation step and radiolabeling to improve the sensitivity [25].

Moreover, few HPLC coupled to fluorescence or to photodiode methods are described. These latter methods allow good precision and accuracy, but require high sample volumes and time demanding analyses [26, 27]. Currently, tandem mass spectrometry (MS/MS) is becoming a valuable tool for the selective analysis of multiple biomarkers due to highly selective multiple reaction monitoring (MRM) in a simultaneous measurement, allowing small sample volumes and shorter analyses [28].

Here, we developed and applied a simple and fast MS/MS method for the study of PDE3 enzyme activity by simultaneously measuring AMP and cAMP. Then, we applied the described method for the evaluation of the inhibitory effect of DF492 on PDE3 activity. Moreover, we reported a computational study to explain the interactions of DF492 at the binding site of PDE3A compared to Milrinone, its parent drug.

Materials and Methods

Synthesis

Compound DF492 was synthesized according to previous procedures reported elsewhere [24]

Chemicals and Reagents

Working standards of AMP and cAMP were obtained from Sigma. The phosphodiesterase enzyme 3A (PDE3A) was purchased from Calbiochem. Ammonium formate (NH_4COOH) and magnesium chloride ($MgCl_2$) were obtained from Sigma-Aldrich, all other chemicals were of LC-MS grade (Sigma-Aldrich).

Tandem Mass Spectrometry Analysis

Sample injection was obtained by using an LC system 2795 Separation Module (Waters CorpMilford, Massachusetts, US), and the chromatography was performed at room temperature using a GromSaphir 110 C_{18} column (3µm Cartrige 60 x 2 mm) connected to a guard column Security Guard Cartrige C_{18} (4 x 2.0 mm) through an isocratic elution for 5 minutes. The mobile phase consisted of 80% H_2O, 20% ACN and 0.2% AF, the flow rate was set at 0.2 mL/min and the injection volume was 20µL.

The LC system was coupled with a High Capacity Ion Traps HCTmass spectrometer (Bruker Daltonics GmbH, Bremen, Germany)through an ESI source operating in positive mode, a 35 nA current was applied on the capillary while nebulizer pressure was set at 40 psi, dry gas was set at 9.0 L/min and dry temperature was set at 365 °C.

Peak detention was performed by MRM of the transitions of m/z 348.2 →136.1 for AMP and m/z 330.1 → 136.1 for cAMP, with a scan time of 0.2 s. The mass scan was set from 50 to 500 m/z, and the fragmentation was performed by using helium as collision gas.

LC-MS/MS method was developed and optimized using a solution of AMP and cAMP 0.1 µmol/mL dissolved in H_2O and ACN 50:50 and 0.2% AF.

Preparation of Stock Solutions and Calibrations Standards

The stock solutions of AMP and cAMP were prepared in 5mM ammonium formate buffer (pH 7.5) and 100 μM of $MgCl_2$ at a concentration of 20 μmol/mL and 10 μmol/mL respectively. A reproducibility test was performed by analysing six replicates of a solution containing cAMP at 3.5 pmol/μL, AMP at 0.25 pmol/μL, DMSO (1 μL) using 5 mM ammonium formate buffer (pH 7.5) and 100 μM of $MgCl_2$ as solvent to achieve a final volume of 200 μL.

A correlation curve was performed using five solutions prepared at increasing concentrations, in particular 0.35, 0.87, 1.75, 2.6, and 3.5 pmol/μL for cAMP and 0.25, 0.32, 0.4, 0.7 and 0.9 pmol/μL for AMP (n=4).

Study of PDE3A Activity and effects of PDE3A Inhibitors

Enzyme activity was investigated by preparing an enzymatic reaction mixture containing 10 μL of PDE3A 0.15 nmol/mL, 1 μL of DMSO, 89 μL of 5mM ammonium formate buffer (pH 7.5) and 100 μM of $MgCl_2$. Reaction was initiated by addition of the substrate molecule (cAMP) at 7.0 nmol/mL (100 μL) and incubated at 37 °C. The reactions were stopped by placing the solutions at 100 °C; then, the samples were centrifuged for 5 minutes at 9280 rcf and stored at -20 °C until further analysis.

Inhibitory action of Milrinone and DF492 was investigated by preparing an enzymatic reaction mixture containing 10 μL of PDE3A 0.15nmol/mL,1 μL of inhibitors at increasing concentrations (20-1200 nM and 20-600 nM, respectively), 89 μL of 5 mM ammonium formate buffer (pH 7.5) and 100 μM of $MgCl_2$. Reaction was initiated by addition of cAMP at 7.0 nmol/mL (100 μL) and incubated at 37 °C. The reactions were stopped, centrifuged and stored as previously reported.

Data Analysis

Mass spectrometry data obtained have been processed by using GraphPad Prism software. The PDE3A activity was determined as a ratio of peak area of AMP (product) and the sum of peak areas of AMP and cAMP (substrates), data were expressed as mean ± standard deviation (SD). Inhibitory actions of DF492 and Milrinone were investigated by performing a non-linear regression using a build-model called dose-response inhibition and by calculating IC_{50} for each inhibitor. Data were expressed as mean ± standard deviation (SD) *versus* logarithm of inhibitors concentration.

Docking Studies

Molecular docking studies toward the human PDE3A have been carried out with the aim of predicting the binding mode of the molecule DF492 and to explain its inhibitory potential. As the crystal solved structure of PDE3A is not available in the Protein Data Bank (PDB), we employed a model recently created and validated by Muñoz-Gutiérrez et al. by using homology modelling and molecular dynamics simulations [29]. This model was generated based on the X-ray structure of the catalytic domain of PDE3B (PDB entry: 1SO2) provided that an identity of 66% was found by considering the catalytic residues from 674 to 1140 of PDE3A *vs* PDE3B. Noteworthy, no differences were observed for those residues with a clear role for binding interactions. This homology model was used as input for the protein preparation wizard, available from the Schrödinger suite [30]. A number of seven water molecules together with the two magnesium ions were kept because of their functional and catalytic functions. Particularly, six out of seven water molecules are crucial for the coordination of the two magnesium ions [29] while the other is involved in a relevant water bridge interaction within the PDE3A binding pocket. Next, the ligand structures to be docked were optimized using the LigPrep tool [31] allowing the generation of the possible ionization states at pH from 6 to 8 as well as all the generation of the possible tautomers. First, the energetic gridbox was centered on the center of mass of PZO14, the cognate ligand of the PDE3B, which included a

dihydropyridazinone ring very similar to the dihydropyridine ring of DF492 and Milrinone, a well-known inhibitor of PDE3 whose X-ray structure is however still missing. The posing of PZO14 and its high similarity to DF492 and Milrinone was used as criteria to drive and assess docking studies.

Glide Standard Precision (SP) was used for docking studies by implementing default settings. The Molecular Mechanics/Generalized Born Surface Area (MM-GBSA) approach was also investigated in order to calculate the binding free energies (ΔG) between protein and ligands [32]. In the MM-GBSA method, the binding free energy (ΔG_{bind}) between the ligand and the target a complex is calculated as:

$$\Delta G_{bind} = \Delta E_{MM} + \Delta G_{pol} + \Delta G_{np}$$

where ΔE_{MM} term includes bond stretching, angle bending, torsion rotation, van der Walls, and electrostatic contributions; ΔG_{pol} term represents the polar contribution to the solvation free energy while the ΔG_{np} term stands for the non-polar contribution. To carry out our analyses, we used Prime package available in the Schrodinger software [31]. Satisfactorily, the top-scored pose of PZO14 carried out from re-docking analysis returned a RMSD value equal to 0.40 Å and docking score and ΔG_{bind} values equal to -12.561 kcal/mol and -109.78 kcal/mol, respectively.

Results and Discussion

Tandem Mass Spectrometry Method Assessment

To determine the amount of AMP and cAMP, two different mass transitions were used for each molecule, as shown in the representative chromatograms and mass spectrum obtained from MS/MS analysis in Figure 2. Panel A and B show chromatogram peak and mass spectrum from AMP and cAMP fragmentation, respectively.

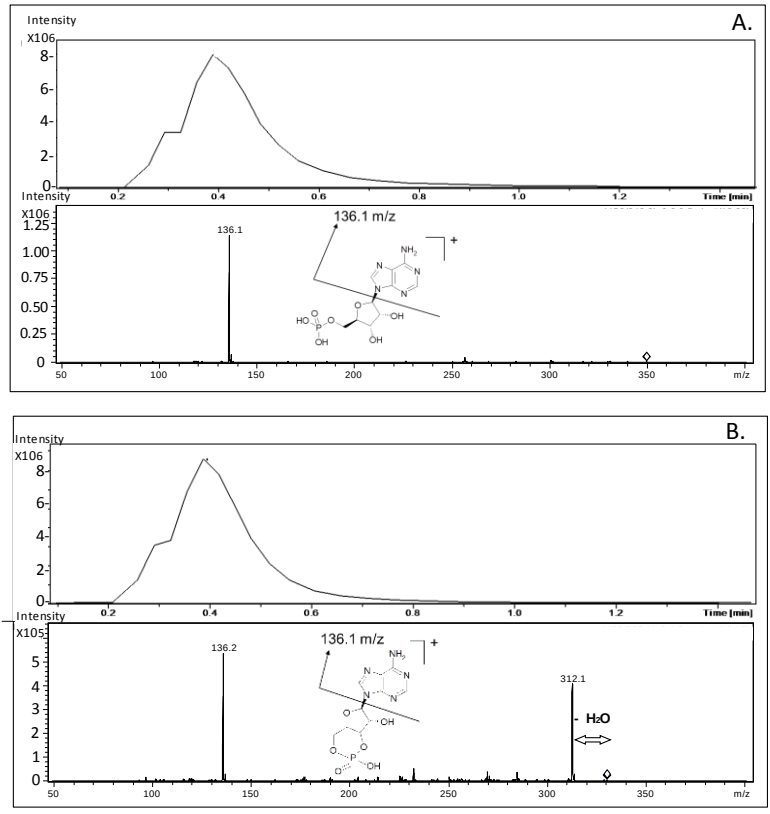

Figure 2: Representative chromatograms and mass spectrum obtained from MS/MS analysis. Panel A and B show chromatogram peaks and mass spectrum from AMP and cAMP fragmentation, respectively.

The proposed method did not provide a chromatographic retention for AMP and cAMP, since the column was exclusively used as in-line filter to limit samples impurities.

To test the method reproducibility we performed a correlation curve by estimating peak areas of AMP and cAMP; data obtained were, then, correlated to their concentrations according to the following formulas: area AMP/(area AMP+ area cAMP) and [AMP]/([AMP] + [cAMP]). Five different solutions (A, B, C, D, E) with increasing concentrations of AMP and decreasing concentrations of cAMP have been used, in particular 0.35, 0.87, 1.75, 2.6, and 3.5 pmol/µL for cAMP and 0.25, 0.32, 0.4, 0.7

and 0.9 pmol/µL for AMP (n=4). As reported in Figure 3, the regression equation was y=1.023x+ 0.134 (R^2= 0.984) indicating good and linear correlation and reproducibility (RSD%< 7.55).

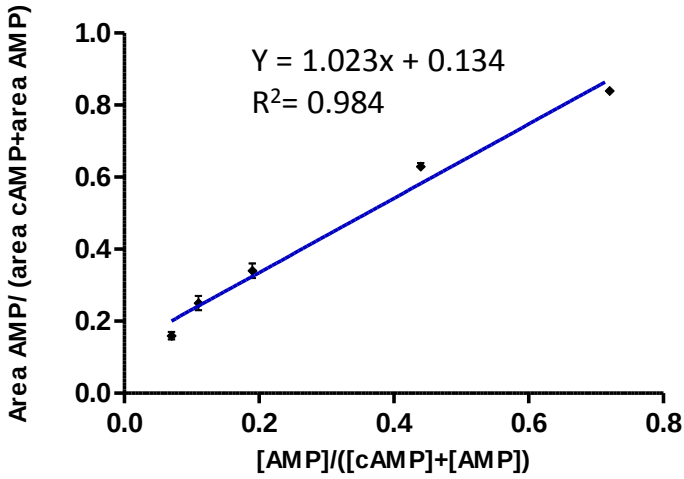

Figure 3: A correlation curve was performed using five solutions prepared at increasing concentrations, in particular 0.35, 0.87, 1.75, 2.6, and 3.5 pmol/µL for cAMP and 0.25, 0.32, 0.4, 0.7 and 0.9 pmol/µL for AMP (n=4).

On the basis of these results, we carried out enzymatic activity studies using the area ratio of the mass signals, regardless of the absolute concentration of AMP and cAMP.

The developed method was applied to the study of PDE3A activity without inhibitors and subsequently with Milrinone and DF492 as inhibitors.

PDE3A activity was investigated performing an experiment by using cAMP at 7 nmol/mL as substrate and PDE3A at 0.15nmol/mL, as described in previous sections. Enzymatic activity was calculated at different time points: 0, 5, 10, 15, and 20 minutes after enzyme incubation. Through the MS/MS method developed, at each point, cAMP (substrate) and AMP (product) peak areas were detected, and the area ratio was calculated. The results are shown by the histogram in Figure 4. Data show that already after 10 minutes of incubation an

appreciable enzymatic activity is present and the RSD% observed has the lowest value (RSD%=1.20). Thus, we decided to observe inhibitors effects on PDE3A activity after 10 minutes of incubation.

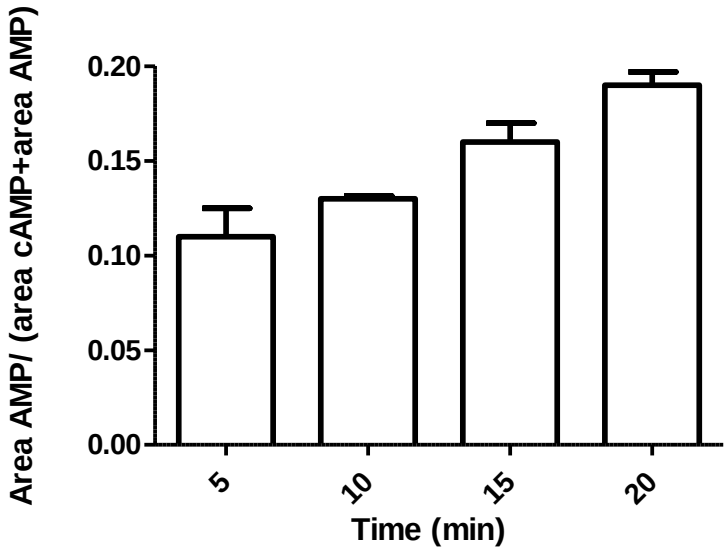

Figure 4: Enzymatic activity evaluated by the ratio of AMP area and AMP+cAMP areas after enzyme incubation at different time points (0, 5, 10, 15, 20 minutes after incubation) (n=3).

Enzymatic Activity with and without Inhibitors

Firstly, Milrinone effect was investigated by performing an experiment at increasing concentrations of the inhibitor (20-1200 nM) and a percentage residual activity was estimated, as reported in Table 1. Three replicates were analysed for each condition and it was considered the average residual activity with the relative SD and RSD%.

Table 1: Residual enzymatic activity % calculated by adding different solutions at increasing concentration of Milrinone, as inhibitor.

[Milrinone](nM)	Residual activity %	SD (n=3)	RSD%
20	90.73	1.03	1.13
200	74.95	1.53	2.04
400	59.62	0.14	0.23
600	47.83	0.84	1.75
1200	43.18	0.97	2.24

Similarly, DF492 inhibitor effect was investigated by using an increasing concentration of the inhibitor (20-600 nM) as reported in Table 2.

Table 2: Residual enzymatic activity % calculated by adding different solutions at increasing concentration of DF492, as inhibitor.

DF492 concentration (nM)	Residual activity %	SD (n=3)	RSD%
20	84.04	4.25	5.05
200	71.75	0.69	0.96
400	53.77	1.65	3.06
600	35.18	2.1	5.97

As reported in Figure 5, we performed a non-linear regression using a "dose-response inhibition" build-model to calculate the concentration of inhibitor that gives a response half way between bottom and top (IC_{50}), by using GraphPad Prism [33].

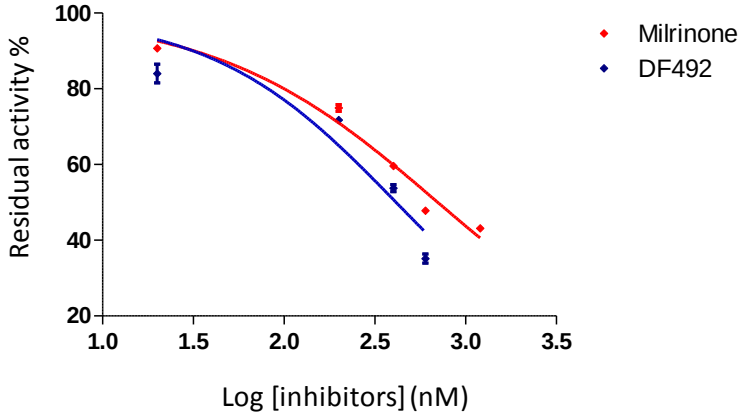

Figure 5: Non-linear regression evaluated by using a "dose-response inhibition" build-model to calculate the concentration of inhibitor that gives a response half way between bottom and top (IC_{50}). The figure shows the residual activity% versus the logarithm of Milrinone (red line) and DF492 (blue line) concentrations and the IC_{50} correlated.

Firstly, we performed a comparison in order to investigate which model fits best, for each data set (Milrinone and DF492 activity). The considered models are "log inhibitors *versus* normalized response" and "log inhibitors *versus* normalized response-variable slope". The first model assumes that the dose-response curve has a standard slope, called Hill slope, of -1.0; the second one does not assume a standard slope but rather fits the Hill Slope from the data, and it is called a Variable slope model. In Table 3 we reported the results obtained from the statistical comparison.

Table 3: Statistical comparison between two models considered: "log inhibitors versus normalized response" and "log inhibitors versus normalized response- variable slope" for each inhibitor. The table lists $LogIC_{50}$ and IC_{50} obtained from the comparison, the HillSlope considered, and the preferred model resulted.

	Milrinone		**DF492**	
	log(inhibitor) vs. normalized response	log(inhibitor) vs. normalized response -- Variable slope	log(inhibitor) vs. normalized response	log(inhibitor) vs. normalized response -- Variable slope
$LogIC_{50}$	2,808	2,847	2,612	2,617
IC_{50}	643,2	703.1	409,5	414,1
HillSlope	-1.0	-0,7113	-1.0	-0,8530
P value	0,0008 (**)		0,6527 (NS)	
Preferred model	log(inhibitor) vs. normalized response -- Variable slope		---	

According to the results obtained for the Milrinone data set, there is a significant difference between the two models (p-value= 0.0008) and the "log inhibitors *versus* normalized response-variable slope" is the preferred one. At contrast, for DF492 data set there is not a significant difference between the two equations (p-value= 0.653), for this reason it was considered the "variable slope-model" for each data set.

Such data processing highlights a significant difference between the two inhibitors considered: Milrinone has an IC_{50} equal to 703.1 nM, while the IC_{50} of DF492 is 409.5nM. These data suggest that DF492 possesses a better PDE3 inhibitory effect than Milrinone. Probably, the replacement of the pyridine with a piperidine ring causes the capability of DF492 to better interact with PDE3.The larger hydrophobic groups of DF492 in place of pyridine of the Milrinone, probably increase the potency of the compound. This observation is consistent with the fact that the ethyl 4-amido-1-piperidine carboxylate substituent could extend into a large hydrophobic pocket; this increase of the size of the group would optimize interactions with the protein [34].

Molecular Docking

To better understand the greater PDE3 inhibitory effect of DF492 compared to Milrinone, a molecular docking study toward the human PDE3A have been carried out with the aim of predicting the binding mode of the DF492 and to explain its inhibitory potential.

Figure 6 shows the binding mode of the top-scored solution of DF492 in PDE3A binding pocket.

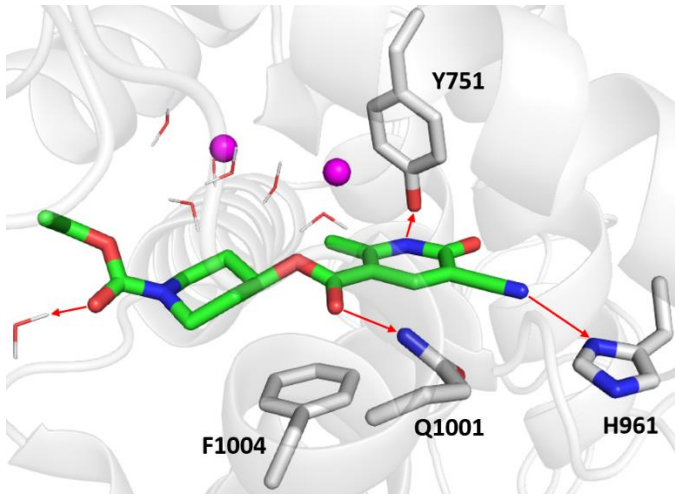

Figure 6: Zoomed in view of the PDE3A binding site. DF492 is rendered in green sticks representation, the most relevant residues are reported as gray sticks, the magnesium ions are indicated as violet spheres, the water molecules are depicted as wireframes. The red arrows indicate the hydrogen bonds.

The docking score and ΔG_{bind} values were equal to -9.007 Kcal/mol and -50.55 Kcal/mol, respectively. As far as DF492 is concerned, the nitrogen atom of the dihydropyridine ring engages a hydrogen bond with the hydroxyl group of Tyr751, the cyano group makes hydrogen bond with side chain of His961, and the carboxyl groups are involved in hydrogen bonds with the side chain of Gln1001 and with a functional water molecule of the binding pocket. Furthermore, a sandwich-like conformation between Phe1004 and the dihydropyrazine ring can be observed

being this very similar to the π-stacking interaction occurring between Phe1004 and the pyridine ring of Milrinone (Figure 7).

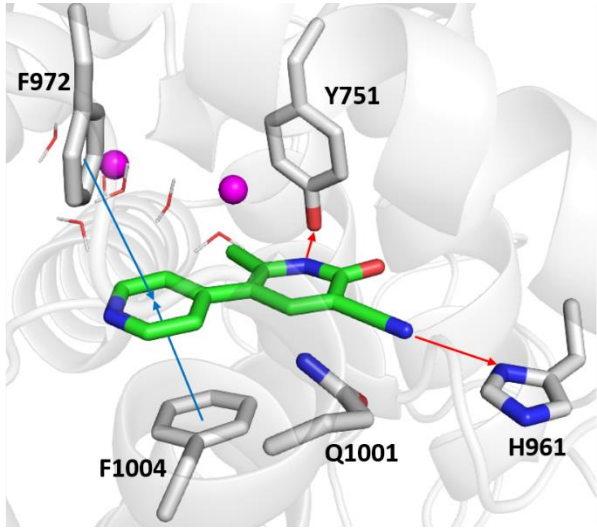

Figure 7: Zoomed in view of the PDE3A binding site. Milrinone is rendered in green sticks representation, the most relevant residues are reported as gray sticks, the magnesium ions are indicated as violet spheres, the water molecules are depicted as wireframes. The red and blue arrows indicate the hydrogen bonds and the π–π interactions.

As shown in Figure 7, the top-scored docking pose of Milrinone was provided with a docking score and ΔG_{bind} value equal to -7.588 Kcal/mol and to -25.79 Kcal/mol, respectively. Likewise DF492, there are two hydrogen bonds engaged by the tri-substituted dihydropyridine ring and the side chains of Tyr571 and His961. In addition, π–π interactions occurred between its pyridine ring with Phe1004 and Phe972. Milrinone can experience hydrophobic interactions with Tyr751, His752, His756, Asp950, Ile951, Asn952, Gly953, Pro954, Lys956, Leu962, Trp964, Thr965, Ile968, Val969, Phe972, Phe989, Met990, Leu1000, Gln1001, Ser1003, Phe1004, Ile1005, Ile1008 and Val1009 being most of these also visited by DF492.

In addition, the affinity is further supported by a network of hydrophobic contacts with Tyr751, His752, His756, Asp950, Ile951, Asn952, Gly953, Pro954, Ala955, Lys956, His961,

Leu962, Trp964, Thr965, Ile968, Val969, Phe972, Gln975, Ser987, Pro988, Phe989, Met990, Leu1000, Gln1001, Ser1003, Phe1004, Ile1005, Ile1008 and Val1009.

The herein reported computational studies shed light on the interactions of DF492 at the binding site of PDE3A. Importantly, the design of DF492 was inspired by Milrinone whose tri-substituted dihydropyridine ring was kept unchanged for anchoring the binding site. On the other side, the inclusion of different decorating bulkier fragments was pursued to shift affinity of DF492 toward PDE3A compared to Milrinone in according to both theoretical and experimental results.

Conclusion

Cyclic nucleotides are intracellular second messengers playing a key role in many physiological processes, in various cell types and tissues. To turn off their signalling, cAMP and cGMP are degradated by PDEs, in particular PDE3is an important regulator of cAMP-mediated responses within the cardiovascular system, with distinct cellular and subcellular locations. Indeed, PDE inhibitors, as Milrinone, have aroused much interest as a group of potential anti-inflammatory and anti-remodeling drugs, since the cardioprotective and neuroprotective effects of the consequent increase of the cAMP are well known [6, 14].

Here, we described an MS/MS method for a fast, cheap, specific and reproducible determination of phosphodiesterase activity through the monitoring of AMP and cAMP levels during catalytic reaction. The developed method was applied to compare two PDE3 inhibitor molecules, as Milrinone and DF492, showing for the latter a greater inhibitory power. This rapid method is extremely simple and reproducible and could be useful for exploratory and preliminary studies aimed at developing deeper tests. In addition, unlike the most MS/MS applications, our method does not require isotopic molecules as internal standards, since the quantification of PDE3 activity includes an internal normalization. Moreover, docking studies show as interactions of DF492 at the binding site of PDE3A can

explain at a molecular level the observed better inhibitory effect with respect to Milrinone.

In summary, we have described a MS/MS approach that could have a wider potential use in kinetic and biomedical studies. Furthermore, the high selectivity of the method could be applied to the study of different activities of phosphodiesterase, potentially used for the determination of other phosphodiesterase inhibitor molecules. Moreover, the computational studies confirmed shift affinity of DF492 toward PDE3A compared to Milrinone in agreement with experimental results.

References

1. Francis SH, Turko IV, Corbin JD. Cyclic nucleotide phosphodiesterases: relating structure and function. Prog Nucleic Acid Res Mol Biol. 2001; 65: 1-52.
2. Fan Chung K. Phosphodiesterase inhibitors in airways disease. Eur J Pharmacol. 2006; 533: 110-117.
3. Sun B, Li H, Shakur Y, Hensley J, Hockman S, et al. Role of phosphodiesterase type 3A and 3B in regulating platelet and cardiac function using subtype-selective knockout mice. Cellular signall. 2007; 19: 1765-1771.
4. Park H, Young Lee S, Lee DS, Yim M. Phosphodiesterase 4 inhibitor regulates the TRANCE/OPG ratio via COX-2 expression in a manner similar to PTH in osteoblasts. Biochem Biophys Res Commun. 2007; 354: 178-183.
5. Ayres JK, Maani CV. Milrinone. StatPearls, Treasure Island (FL). 2019.
6. Jung HS, Joo JD, Kim DW, In JH, Roh M, et al. Effect of milrinone on the inflammatory response and NF-kB activation in renal ischemia-reperfusion injury in mice. Korean J Anesthesiol. 2014; 66: 136-142.
7. Besirli K, Burhani SM, Arslan C, Suzer O, Sayin AG. Effect of combining phosphodiesterase III inhibitors with St Thomas Hospital's solution used as transplantation preservative solution in isolated rat hearts. Transplant Proc. 2006; 38: 1253-1258.
8. Zhang J, Chen F, Zhao X, Aoyama A, Okamoto T, et al. Nebulized phosphodiesterase III inhibitor during warm

ischemia attenuates pulmonary ischemia-reperfusion injury. The Journal of heart and lung transplantation : the official publication of the International Society for Heart Transplantation. 2009; 28: 79-84.
9. Satoh K, Kume M, Abe Y, Uchinami H, Yakubouski SV, et al. Implication of protein kinase A for a hepato-protective mechanism of milrinone pretreatment. J Surg Res Title. 2009; 155: 32-39.
10. Uysal E, Dokur M, Altinay S, Saygili EI, Batcioglu K, et al. Investigation of the Effect of Milrinone on Renal Damage in an Experimental Non-Heart Beating Donor Model. Journal of investigative surgery : the official journal of the Academy of Surgical Research. 2018; 31: 402-411.
11. Lanfear DE, Hasan R, Gupta RC, Williams C, Czerska B, et al. Short term effects of milrinone on biomarkers of necrosis, apoptosis, and inflammation in patients with severe heart failure. J Transl Med. 2009; 7: 67.
12. White M, Ducharme A, Ibrahim R, Whittom L, Lavoie J, et al. Increased systemic inflammation and oxidative stress in patients with worsening congestive heart failure: improvement after short-term inotropic support. Clin sci. 2006; 110: 483-489.
13. de Miranda ML, Pereira SJ, Santos AO, Villela NR, Kraemer-Aguiar LG, et al. Milrinone attenuates arteriolar vasoconstriction and capillary perfusion deficits on endotoxemic hamsters. PloS one. 2015; 10: e0117004.
14. Saklani R, Jaggi A, Singh N. Pharmacological preconditioning by milrinone: memory preserving and neuroprotective effect in ischemia-reperfusion injury in mice. Arch Pharm Res. 2010; 33: 1049-1057.
15. Crespy T, Heintzelmann M, Chiron C, Vinclair M, Tahon F, et al. Which Protocol for Milrinone to Treat Cerebral Vasospasm Associated With Subarachnoid Hemorrhage? J Neurosurg Anesthesiol. 2019; 31: 323-329.
16. Al-Jehani H, Angle M. Intravenous Milrinone Salvage Therapy in Acute Internal Carotid Artery Occlusion: Case Report. Neurol and ther. 2019; 8: 161-165.
17. Dorigo P, Gaion RM, Belluco P, Mosti L, Borea PA, et al. An analysis of the mechanism of the inotropic action of

some milrinone analogues in guinea-pig isolated atria. Br J Pharmacol. 1991; 104: 867-872.
18. Fossa P, Boggia R, Lo Presti E, Mosti L, Dorigo P, et al. Inotropic agents. Synthesis and structure-activity relationships of new milrinone related cAMP PDE III inhibitors, Farmaco. 1997; 52: 523-530.
19. Floreani M, Fossa P, Gessi S, Mosti L, Borea PA, et al. New milrinone analogues: in vitro study of structure-activity relationships for positive inotropic effect, antagonism towards endogenous adenosine, and inhibition of cardiac type III phosphodiesterase. N-S Arch Ph. 2003; 367: 109-118.
20. Krauze A, Vitolina R, Garaliene V, Sile L, Klusa V, et al. 3,4-trans-4-Aryl-3-(1-pyridinio)-1,2,3,4-tetrahydropyridine-6-thiolates--new group of potential cardiotonic drugs, Eur J Med Chem. 2005; 40: 1163-1167.
21. de Candia M, Fossa P, Cellamare S, Mosti L, Carotti A, et al. Insights into structure-activity relationships from lipophilicity profiles of pyridin-2(1H)-one analogs of the cardiotonic agent milrinone. Eur J Pharm Sci. 2005; 26: 78-86.
22. Mosti L, Menozzi G, Schenone P, Dorigo P, Gaion RM, et al. Synthesis and Cardiotonic Activity of Esters of 2-Substituted 5-Cyano-1,6-Dihydro-6-Oxo-3-Pyridinecarboxylic Acids - Crystal-Structure of 2-Methyl, 2-Tert-Butyl and 2-Phenyl Esters. Eur J Med Chem. 1989; 24: 517-529.
23. Cody V, Wojtczak A, Davis FB, Davis PJ, Blas SD. Structure-Activity-Relationships of Milrinone Analogs Determined in-Vitro in a Rabbit Heart Membrane Ca2+-Atpase Model. J Med Chem. 1995; 38: 1990-1997.
24. Pietrangelo T, Giampietro L, De Filippis B, La Rovere R, Fulle S, et al. Effect of milrinone analogues on intracellular calcium increase in single living H9C2 cardiac cells. Eur J Med Chem. 2010; 45: 4928-4933.
25. Torremans A, Ahnaou A, Van Hemelrijck A, Straetemans R, Geys H, et al. Effects of phosphodiesterase 10 inhibition on striatal cyclic AMP and peripheral physiology in rats. Acta Neurobiol Exp. 2010; 70: 13-19.

26. Matencio A, Garcia-Carmona F, Lopez-Nicolas JM. An improved "ion pairing agent free" HPLC-RP method for testing cAMP Phosphodiesterase activity. Talanta. 2019; 192: 314-316.
27. Diaz Enrich MJ, Villamarin JA, Ramos Martinez JI, Ibarguren I. Measurement of adenosine 3',5'-cyclic monophosphate and guanosine 3', 5'-cyclic monophosphate in mussel (Mytilus galloprovincialis lmk.) by high-performance liquid chromatography with diode array detection. Anal biochem. 2000; 285: 105-112.
28. Oeckl P, Ferger B. Simultaneous LC-MS/MS analysis of the biomarkers cAMP and cGMP in plasma, CSF and brain tissue. J Neurosci Methods. 2012; 203: 338-343.
29. Munoz-Gutierrez C, Caceres-Rojas D, Adasme-Carreno F, Palomo I, Fuentes E, et al. Docking and quantitative structure-activity relationship of bi-cyclic heteroaromatic pyridazinone and pyrazolone derivatives as phosphodiesterase 3A (PDE3A) inhibitors. PloS one. 2017; 12: e0189213.
30. Schrödinger Release 2018-2: Schrödinger Suite 2018-2 Protein Preparation Wizard.
31. LigPrep, Schrödinger. 'LLC.' New York. 2018.
32. Genheden S, Ryde U. The MM/PBSA and MM/GBSA methods to estimate ligand-binding affinities. Expert opin on drug dis. 2015; 10: 449-461.
33. Chen Z, Bertin R, Froldi G. EC50 estimation of antioxidant activity in DPPH. assay using several statistical programs. Food Chem. 2013; 138: 414-420.
34. Scapin G, Patel SB, Chung C, Varnerin JP, Edmondson SD, et al. Crystal structure of human phosphodiesterase 3B: atomic basis for substrate and inhibitor specificity. Biochem. 2004; 43: 6091-6100.